

사파이어 단결정의 basal (0001) 결정면에 미세압흔시 온도에 따른 압흔 주위 미세구조에 관한 연구

윤 석 영

부산대학교 공과대학 무기재료공학과

The Substructure Near Indents With Temperature During Microindentation on Basal (0001) Plane in Sapphire Single Crystals

Seog-Young Yoon

Department of Inorganic Materials Engineering at Pusan National University,
30 Changjung-Dong, Kumjung-Gu, Pusan, 609-735

(2000년 8월 1일 받음, 2000년 10월 6일 최종수정본 받음)

초 특 사파이어 단결정 basal 결정면을 이용 상온에서 1000°C 범위내에서 온도에 따른 Vickers 미세경도를 측정하였다. 화학적 연마, 에칭, 광학현미경 그리고 투과전자현미경 (TEM) 을 이용하여 압흔주위의 미세구조에 대하여 검토하였다. 상온에서는 균열이 지배적이었으며, 중간온도 (400°C and 600°C) 에서는 많은 rhombohedral 쌍정이 관찰되었다. 한편, 고온에서는 prism 면상에 prism slip bands가 미세구조상에서 지배적이었다. TEM을 통해 압흔주위의 전위들은 basal 면과 prism 면상에 존재하며, Burgers 벡터가 $\langle 1100 \rangle$ 과 $\langle 1120 \rangle$ 인 것으로 판명되었다. $\langle 1100 \rangle$ 나선전위가 prism 면상에서 세 개의 부분전위 $1/3 \langle 1100 \rangle$ 로 분해됨과 사파이어 단결정의 Peierls potential에 대하여 검토되었다.

Abstract The Vickers microhardness was measured on the basal (0001) plane of sapphire single crystals in the temperature range from 25°C to 1000°C. The substructure surrounding the indents was investigated using selective chemical polishing and etching, optical microscopy, and transmission electron microscopy (TEM). At room temperature, cracks were predominant, and at intermediate temperatures (400°C and 600°C), extensive rhombohedral twinning was observed. On the other hand, at higher temperatures, prism plane slip bands on prism plane $\{1120\}$ were dominant in the microstructure. TEM observations revealed that the dislocation substructure at the vicinity of the indents consisted of fairly straight dislocations lying in basal and /or prism planes and aligned along the $\langle 1100 \rangle$ and $\langle 1120 \rangle$ directions. The details of the glide dissociation of perfect $\langle 1100 \rangle$ screw dislocations into three collinear $1/3 \langle 1100 \rangle$ partials on the prism plane and the Peierls potential for sapphire single crystals were discussed.

Key words : Sapphire Single, crystals, etching, Microindentation

1. Introduction

Sapphire has thermodynamic stability and relatively high melting point so that makes it a promising candidate for structural materials in oxidizing environment, and for single crystal fiber reinforcements in advanced composite ceramics. During high temperature plastic deformation of sapphire, the yield stress of particular slip system varies with temperature.¹⁾

To understand the changes with variations of the temperature, plastic deformation of sapphire single crystals have been studied in detail using constant strain rate deformation^{2~4)}, creep and fracture test^{5,6)} after Kronberg⁷⁾ predicted that slip and twinning to be important modes of plastic deformation mechanism of

sapphire at elevated temperatures. A number of investigators^{8~11)} have determined the primary slip systems at high temperatures, work-hardening and dynamic recovery and creep.

In recent years, microhardness studies, which has been shown to be useful to investigate the deformation behavior of brittle materials, have been used to study the micro-plastic behavior around microhardness indents at room temperature^{1,2)} and at high temperatures.¹³⁾ It has been shown that dislocation plasticity can occur even at room temperature and that the slip systems varied with temperature.

This study is aimed to characterize the substructure of the plastic zone formed during indentation on the basal plane of sapphire single crystals in the tempera-

ture range from room temperature to 1000°C. A combination of chemical polishing and etching, in conjunction with optical and transmission electron microscopy, was employed to systematically investigate the generation and motion of dislocations and deformation twins.

2. Experimental procedure

Ingots of Czochralski grown undoped sapphire single crystals were obtained from a commercial source. Specimens were analysed by the Laue back-reflection X-ray technique and cut using a diamond saw in the dimension $10 \times 5 \times 3 \text{ mm}^3$. Basal (0001) planes were polished with different grades of diamond paste, finishing with a $1 \mu\text{m}$ grade and then Syton (a colloidal silica slurry). Indentations were made with a Vickers diamond indenter using a hot hardness tester under 10^{-5} torr vacuum. Specimens for etching experiments were indented with 200 gram loads using a dwell time of 15 sec at various temperatures.

Indented samples were etched in a saturated solution of KOH at 400°C for 10 to 15 min. For chemical polishing, boiling H_3PO_4 at 420°C was used. The surface of the samples after indentation and etching was investigated using Normarski interference microscopy and Tolanski interferometry.

For TEM analysis, 3 mm diameter disks were cut using an ultrasonic drill, which were then indented with

a 200 gram load using a dwell time of 5 sec. These disks were subsequently ground to $100 \mu\text{m}$ thickness from the side opposite to the indented surface and dimpled to a depth of $20 \mu\text{m}$. The samples were back-thinned in an conventional ion mill and were coated with carbon prior to TEM investigation using a JEOL 200CX electron microscope.

3. Results

The temperature dependence of the microhardness is shown in Fig. 1. The hardness decreased with increasing temperature and the absolute values were close to

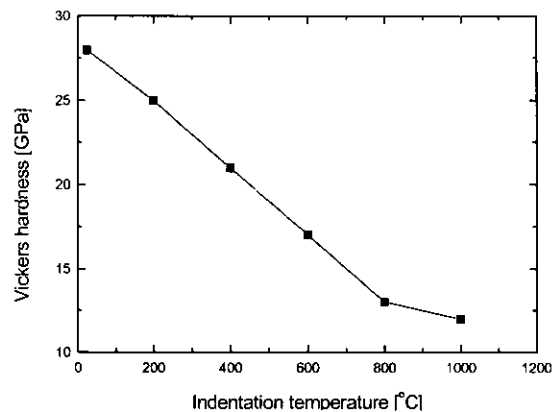


Fig. 1. Temperature dependence of the Vickers microhardness on the basal plane of sapphire single crystals at 200g indentation load.

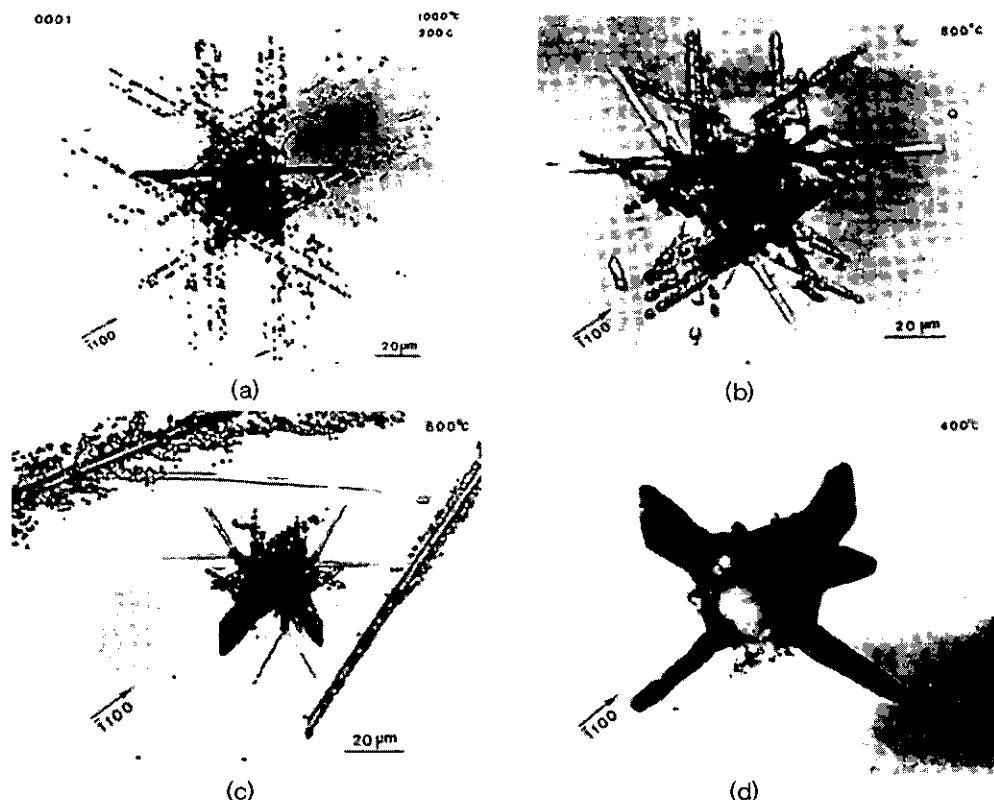


Fig. 2. Etched substructure of the plastic zone at vicinity of a Vickers indent on the basal (0001) plane at different temperatures. (a) 1000°C, (b) 800°C, (c) 600°C, and (d) 400°C.

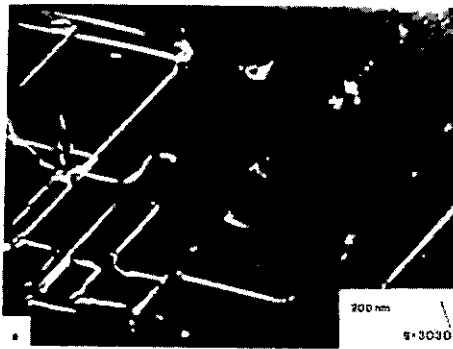


Fig. 3. Dark-field image of two sets of the screw dislocations lying on $\{11\bar{2}0\}$ prism planes (marked as S_1 and S_2) viewed to the $[0001]$ direction.

those observed by Kollenberg.¹³⁾

The etched structure of the plastic zone near an indent on the basal plane made at 1000°C under a 200 gram load is shown in Fig. 2(a). The deformation substructure is strongly anisotropic and consists of straight arrays of dislocation etch pits along $\langle 11\bar{0}0 \rangle$ directions, and a homogeneously etched trace along $\langle 11\bar{2}0 \rangle$ due to deformation twinning. Slip trace analysis has shown that these features correspond to slip on $\langle 11\bar{2}0 \rangle$ planes and twinning on $\{10\bar{1}2\}$ planes, respectively.

Chemical polishing and re-etching revealed that after removal of a $30\mu\text{m}$ surface layer, the dislocation arrays were along the initial traces, which confirms that the dislocation arrays lie on planes perpendicular to (0001) . Furthermore, no surface steps from dislocation slip were revealed on the (0001) plane, using either Normarski contrast or Tolanski interferometry, which indicates that the Burgers vectors of the dislocations are parallel to the indentation surface. This set of data allows an unambiguous identification of slip system as $\{11\bar{2}0\} \langle 11\bar{0}0 \rangle$.

As shown in Fig. 2(b), the extent of the plastic zone at 800°C diminished but the relative size of the twin lamellae increased in comparison with that of dislocation slip bands in Fig. 2(a), while at an intermediate temper-

ature of 600°C , twinning dominated the structure as shown in Fig. 2(c). On the other hand, below 400°C , cracks were the main features in the plastic zone of the (0001) indents as seen from Fig. 2(d).

TEM observations revealed details of the deformation processes taken place on a micro scale. The dislocation substructure in a (0001) foil after 1000°C indentation is shown in Fig. 3. Two sets of screw dislocations (S_1 and S_2) lying parallel to the foil surface can be seen. The screw dislocations are aligned almost exactly along $\langle 10\bar{1}0 \rangle$ directions and have Burgers vector orthogonal to the surface normal. Tilting and dislocation line trace analysis experiments revealed that the dislocations lie on the $\{11\bar{2}0\}$ prism planes, which confirms the optical observations. Two weak beam dark field (WBDF) images of dislocations belonging to the $\{11\bar{2}0\}$ slip system are shown in Fig. 4(a) and (b). Fig. 4(a) was obtained by tilting the foil around a $[1100]$ axis by $\approx 30^\circ$. Dislocations in the prism plane are dissociated into three collinear partials, each with $1/3[1100]$ Burgers vectors. Fig. 4(b) was obtained using the same diffraction conditions but closer to the $[0001]$ pole, so that dislocations were viewed almost parallel to prism slip plane. As can be seen in Fig. 4(a) and (b), the screw dislocations consist almost entirely of segments which have cross slipped from the prism plane onto the basal plane. Moreover, each cross slip event (Fig. 4b) corresponds to a constriction (Fig. 4a).

Basal slip was also activated underneath the indent. Fig. 5 shows dark field images of the dislocation structure in the basal plane (parallel to foil surface); conventional $g \cdot b$ analysis revealed that the Burgers vectors of the dislocations in these arrays were $[1120]$.

4. Discussion

Crystallographically-aligned dislocations in the basal and prism slip planes may be considered as the influence of the Peierls potential on dislocation motion in sapphire. The structure of sapphire has been lucidly

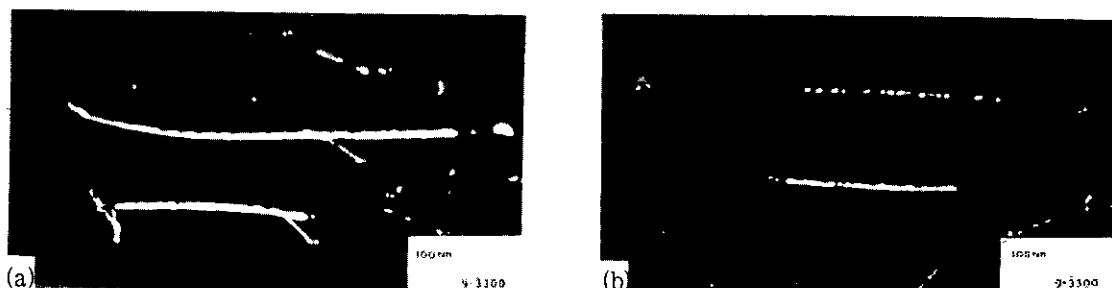


Fig. 4. Weak-beam dark field images of dislocations belonging to the $\{11\bar{2}0\}$ slip system (a) inclined at 30° to the prism plane and (b) parallel to the prism plane.

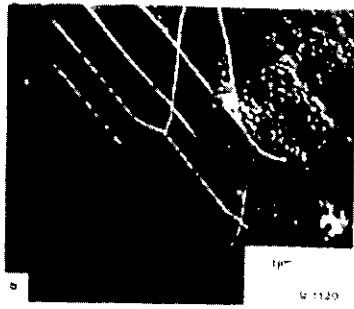


Fig. 5. Dark field images of the dislocation structure in the basal plane. Dislocations are aligned along to $\langle 1120 \rangle$ Burgers vector.

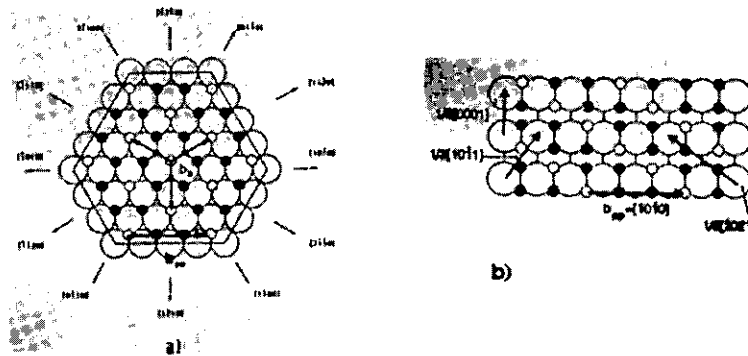


Fig. 6. Arrangement of Al ions (filled circles) oxygen ions (large open circles) in sapphire single crystals. (a) basal plane and (b) prism slip plane. Several possible Burgers vectors for dislocations are also shown.

or electrostatic in origin. In the substructure of the plastic zone near indents made at 1000 °C, the dislocations along $\langle 11\bar{0}0 \rangle$ and $\langle 11\bar{2}0 \rangle$ directions were observed. It thus appears that Peierls barriers along these directions are high enough to affect dislocation motion, even at temperatures as high as $T \approx 0.55 T_m$ ($T_m \approx 2000$ °C).

It is well known that the Peierls stress (τ_p) is related to the absolute value of Burgers vector (b) and the distance between glide planes (d) as like equation (1)¹⁴

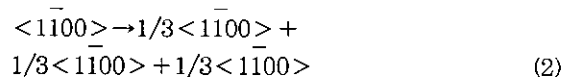
$$\tau_p = \frac{2\mu}{1-\nu} \exp\left(-\frac{4\pi d}{b}\right) \quad (1)$$

where ν is the Poisson ratio and μ is the shear modulus. Possible Burgers vector for the basal and prism dislocations are shown as arrows in Fig. 6 (a) and (b). As mentioned above, the shortest Burgers vector for dislocations in the basal plane corresponds to $b_b = 1/3 \langle 11\bar{2}0 \rangle$ with $|b| = 0.475 nm$. Screw dislocations with the Burgers vector $b_{pp} = \langle 1100 \rangle$ can in principle glide on either the basal or prism plane; they have much higher absolute values of the Burgers vector, $|b| = 0.822 nm$. According to equation (1) the Peierls stress for the

described by Kronberg.⁷ The arrangement of the aluminium and oxygen atoms on the basal (0001) and $\{11\bar{2}0\}$ prism planes are shown in Fig. 6(a) and (b), respectively. Filled circles are Al ions, small open circles denote the unoccupied octahedral interstitial sites, and oxygen ions are shown as large open circles.

As shown in Fig. 6 (a), there are the rational directions; $\langle 11\bar{0}0 \rangle$ corresponds to the close-packed arrays of oxygen atoms in the anion sublattice, while $\langle 11\bar{2}0 \rangle$ represents the directions of vacant and filled sites in the cation sublattice. Both of these directions can provide periodic barriers for dislocation motion, whether elastic

motion of $\langle 11\bar{0}0 \rangle$ type dislocations should be higher than that for $1/3 \langle 11\bar{2}0 \rangle$ dislocations. At first sight, this can explain the exact alignment of the screw dislocations along $\langle 11\bar{0}0 \rangle$, which is seen in Fig. 4. However, $\langle 11\bar{0}0 \rangle$ type dislocations can reduce their energy and high Peierls potential by dissociation into three collinear partials according to the reaction¹⁵



This type of glide dissociation of prism plane dislocations can be seen in Fig. 4. As seen from Fig. 4, the lengths of dissociated edge or mixed dislocations are short in comparison with those of constricted screws. This can be interpreted as the indication that the velocities of the dissociated dislocations are higher. Although the high mobility of the dissociated dislocations is in agreement with the expected lower values of the Peierls potential, the low mobility of the screw dislocations and their almost exact alignment along $\langle 11\bar{0}0 \rangle$ directions are determined by the details of their dissociation

into three collinear partials, and local pinning by cross slip onto the basal plane.

5. Conclusions

The substructure of the plastic zone adjacent to microindentations on the basal plane of sapphire in the temperature range from 25°C to 1000°C was characterized using selective chemical etching, optical microscopy, and TEM. At high temperatures (800°C and 1000°C) microplasticity occurred primarily by dislocation slip on the prism plane systems $\{11\bar{2}0\} \langle 1100 \rangle$; at intermediate temperatures (400°C and 600°C) rhombohedral twinning on the $\{10\bar{1}2\}$ planes dominated the substructure, and at low temperatures (below 400°C), cracking was most prevalent. TEM observations in the basal planes after high-temperature indentation suggested a strong influence of the Peierls potential on dislocation motion at temperatures as high as $\approx 0.55 T_m$. Glide dissociation of the $\langle 1100 \rangle$ dislocations into three collinear partials was observed on the prism planes. A correlation between constrictions in dissociated dislocations and cross slip and climb was revealed.

References

1. T.E. Mitchell, K.P.D. Lagerlöf and A.H. Heuer, "Dislocations in Ceramics." in *Materials Science and Technology*, **1**, 349-358 (1985).
2. J. Cadoz, J. Castaing and S.H. Kirby, "Prismatic Slip of Al_2O_3 Single Crystals below 1000°C in Compression Under Hydrostatic Pressure." *J. Am. Ceram. Soc.*, **64**, 504 (1981).
3. M.L. Kronberg, "Dynamical Flow Properties of Single Crystals of Sapphire, I." *J. Am. Ceram. Soc.*, **45** (6), 274-279 (1962).
4. H. Conrad, G. Stone and K. Janowski, "Yielding and Flow of Sapphire ($\alpha-Al_2O_3$) crystals in Tension and Compression." *Trans. AIME*, **233** (5), 889-897 (1965).
5. R. Chang, "Creep of Al_2O_3 Single crystals." *J. Appl. Phys.*, **31** (3), 484-487 (1960).
6. P.F. Becher, "Fracture-Strength Anisotropy of Sapphire." *J. Am. Ceram. Soc.*, **59** (1), 59 (1976).
7. M.L. Kronberg, "Plastic deformation of single crystals of sapphire: Basal slip and Twinning", *Acta Metall.*, **5** (9), 507 (1957).
8. D.J. Gooch and G.W. Groves, "Prismatic slip in sapphire", *Acta Metall.*, **55** (2), 105 (1972).
9. J.D. Snow and A.H. Heuer, "Slip systems in Al_2O_3 ", *J. Am. Ceram. Soc.*, **56** (3), 153 (1973).
10. B.J. Pletka, A.H. Heuer, and T.E. Mitchell, "Work-hardening in sapphire", *Acta Metall.*, **25**, 25 (1977).
11. B.J. Pletka, T.E. Mitchell, and A.H. Heuer, "Dislocation structures in sapphire deformed by Basal slip", *J. Am. Ceram. Soc.*, **57** (9), 388 (1974).
12. H.M. Chan and B.R. Lawn, "Indentation deformation and fracture of sapphire", *J. Am. Ceram. Soc.*, **71** (1), 29 (1988).
13. W. Kollenberg, "Plastic deformation of Al_2O_3 single crystals by indentation at temperatures up to 750°C", *J. Mater. Sci.* **23** (1988).
14. J.P. Hirth and J. Lothe, "Theory of Dislocations" (New York: McGraw-Hill) 1982
15. K.P.D. Lagerlöf, A.H. Heuer, J. Castaing, J.P. Riviere and T.E. Mitchell, "Slip and Twinning in Sapphire ($\alpha-Al_2O_3$)", *J. Am. Ceram. Soc.*, **77** (2), 385-397 (1994).